Fuel 203 (2017) 128–134

Contents lists available at ScienceDirect

Fuel

journal homepage: www.elsevier.com/locate/fuel

Full Length Article

Effective and regenerable Ag/graphene adsorbent for Hg(II) removal from aqueous solution

Zan Qu *, Li Fang, Dongyao Chen, Haomiao Xu, Naiqiang Yan

School of Environmental Science and Engineering, Shanghai Jiao Tong University, 800 Dongchuan Road, Shanghai 200240, China

HIGHLIGHTS

- Ag^{+} and graphene oxide (GO) were co-reduced through simple method.
- The removal efficiency was higher than 99% under the pH of 5.0.
- The co-existed metal ions had hardly impact for the removal.
- The sorbent showed excellent performance of regeneration and reutilization.

GRAPHICAL ABSTRACT

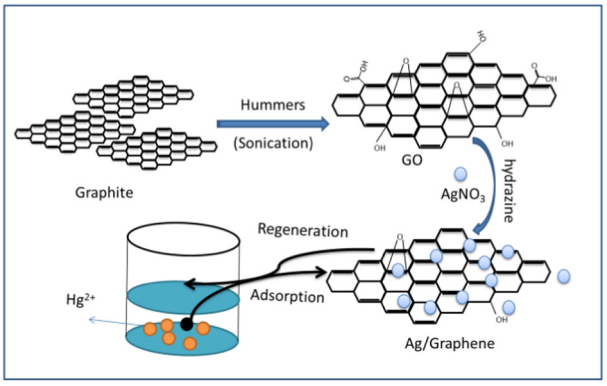

ARTICLE INFO

Article history:
Received 21 December 2016
Received in revised form 17 March 2017
Accepted 24 April 2017

Keywords:
Hg^{2+}
Adsorbent
Graphene
Silver
Regeneration

ABSTRACT

A novel Ag/graphene adsorbent was synthesized for the Hg(II) removal from waste water. The Ag/graphene was characterized by Fourier Transformation Infrared Spectrum (FT-IR), X-ray Diffraction (XRD), Transmission Electron Microscope (TEM) and Scanning Electron Microscope (SEM) devices. The results showed that graphene acted as a good support for Ag particles on its huge surface. The removal efficiency of Hg^{2+} was higher than 98% after 120 min adsorption. The optimized pH value was 5.0. There are no obvious effects of co-existed metal ions (Mn^{2+}, Mg^{2+}, Ca^{2+}, Al^{3+} and Na^{+}) on Hg^{2+} removal. Meanwhile, the adsorption isotherms and adsorption kinetics were applied to analyze the experimental data. The best interpretation was given by Freundlich isotherm equation. The kinetic adsorptions were well described by a pseudo-second-order reaction model. Furthermore, the performance of regeneration and reutilization were also investigated. The results indicated that the adsorption capacity remained stable after 6 reuse cycles.

1. Introduction

Mercury pollution has attracted lots of attention for decades because of its high toxicity and bioaccumulation [1]. With the agreement of the Minamata Convention on Mercury, it becomes more urgent to reduce the mercury emission [2]. Industrial wastewater is one of the major mercury anthropogenic emission sources [3]. Therefore, it is significant to reduce mercury emission from wastewater. Many technologies were used for mercury removal from wastewater such as adsorption, ion exchange, amalgamation and membrane separation [4–7]. Among them, adsorption method is considered as an effective technique because of its simplicity and cost effectiveness [8]. While, the adsorption

* Corresponding author.
E-mail address: quzan@sjtu.edu.cn (Z. Qu).

http://dx.doi.org/10.1016/j.fuel.2017.04.105
0016-2361/

capacity and the regeneration performance of sorbents are still not satisfied. Biomass material and metal oxides were selected as mercury sorbent. However, they often meet the problems of difficult to recycle and low adsorption capacity [9,10]. Thus, it is important to develop novel Hg^{2+} removal sorbent which have high removal efficiency and can be recycled after adsorption [11].

Silver used as an effective sensor for detecting Hg^{2+} in aqueous solution [12]. Many materials have been evaluated for the capture of mercury from fluids such as gas streams like flue gas and syngas [13,14], and the noble metals have shown great promise as sorbents [15–19]. Meanwhile, silver amalgam was often applied for dental filling. It should be a good sorbent for the mercury removal from waste water. However, its application was limited due to its small surface area. This problem can be solved with the development of graphene. As the thinnest and strongest material, graphene is believed to be one of the most potential materials [20]. In recent years, graphene-based materials have aroused extensive attentions and they have been widely studied in many fields [21,22]. Its large surface area provides potential possibility as a good support for mercury sorbent. Therefore, it is desired that Ag particles synthesized on the surface of graphene could be useful for the removal of Hg^{2+} in aqueous solution.

Here, we report a simple approach to prepare the graphene supported Ag materials. The Ag particles and graphene oxide were co-reduced through hydrothermal reaction. The prepared Ag/graphene was used as an effective sorbent for Hg^{2+} removal from aqueous solution. The thermodynamic and kinetic models were used to examine its adsorption performance. Furthermore, the mercury desorption performance was also investigated. It is a promising sorbent for mercury removal and regeneration of sorbent after mercury adsorption.

2. Experimental methods

2.1. Preparation of GO and the Ag/Graphene composites

Graphene oxide (GO) was synthesized from graphite powder based on the Hummers method [23]. GO was formed through low temperature, medium temperature and high temperature period, respectively. 1) Low temperature period: Firstly, 2 g graphite power and 1 g $NaNO_3$ were mixed with 50 mL of 98% H_2SO_4 with stirring for 1 h. Then 0.3 g $KMnO_4$ was added into the mixture with stirring. Thirty minutes later, 7 g of $KMnO_4$ was gradually added into the mixture in 1 h. During this period, the temperature of the mixture was kept below 5 °C. 2) Medium temperature period: The mixture solution was heated to 35–40 °C and stirred for another 2 h. After that, 90 mL of deionized water was introduced into the mixture solution in 15 min. 3) High temperature period: 55 mL of deionized water and 10 mL of H_2O_2 were added into the mixture solution, respectively. Then, the mixture solution was filtrated and washed by 10% HCl solution and deionized water for 4 times, respectively. The product was kept drying at 80 °C for 48 h. 200 mg graphite oxide was added to 200 mL deionized water. Ammonia was used to adjust the pH value of 7.0. The above mixture (2 mg·mL^{-1}) was under ultrasonic for 1 h followed by high-speed stirring for a further 1 h to generate GO.

As shown in Fig. 1, 200 mg of $AgNO_3$ was dissolved in 15 mL of ethyl alcohol with 5 mL of H_2O. Then 100 mL GO was added to the mixture with stirring for 10 h. Then, a certain amount of hydrazine hydrate was added and the mixture solution was heated at 90 °C for 12 h. When the reduction reaction was finished, the resulting

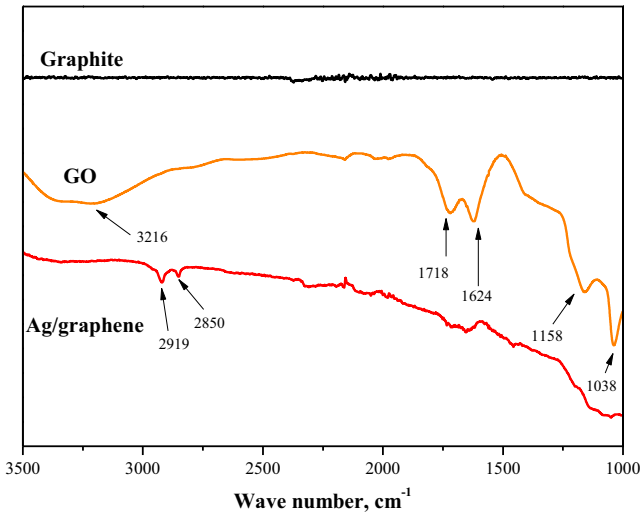

Fig. 2. FT-IR spectra of graphite, GO and Ag/graphene.

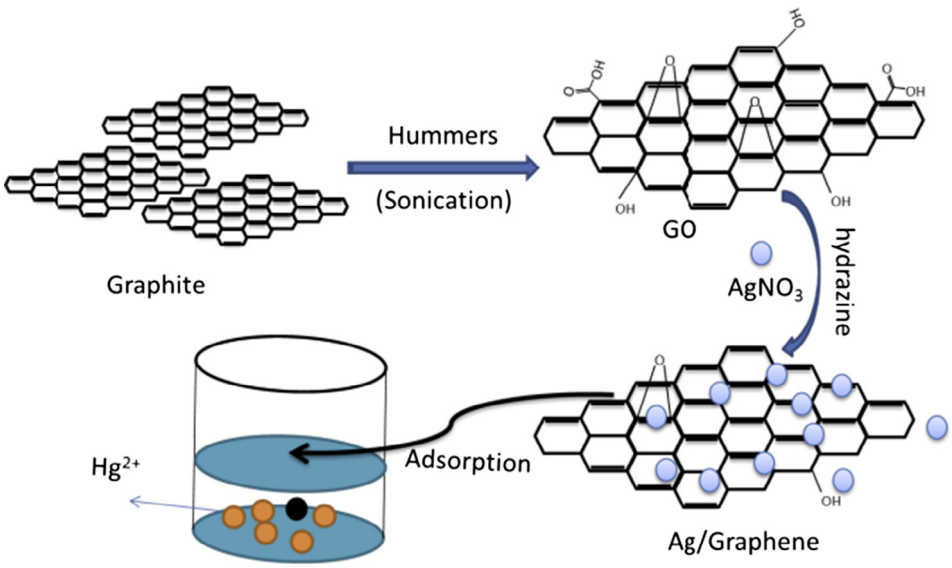

Fig. 1. The synthesis process of Ag/graphene adsorbent.

mixture was filtrated and the product dried in an oven at 100 °C for 5 h. After that, it was transferred to a muffle furnace and calcined at 250 °C for 5 h.

2.2. Characterization

Fourier Transform Infrared spectroscopy (FT-IR) was performed over the wavenumber range of 3500–1000 cm^{-1} to characterize the surface properties. The micrographs were obtained in the bright-field imaging mode at an acceleration voltage of 200 kV. Powder X-ray diffraction patterns were recorded from 10 to 80 degree with scanning velocity of 5 degree min^{-1} on a X-ray Diffractometer (APLX-DUO, BRUKER, Germany) using Cu-K radiation (40 kv and 20 mA). The microstructure of the sorbent was analyzed by Transmission Electronic Microscopy (TEM). TEM image was performed on a JEOLJEM-2010 TEM. The surface morphology was studied by a Scanning Electron Microscope (SEM) (Hitachi Corp., Japan) after gold was coated on the surface. The N_2 sorption measurement was performed using Nova-2200 e, and the specific surface area was calculated using the Brunauer–Emmett–Teller (BET) method.

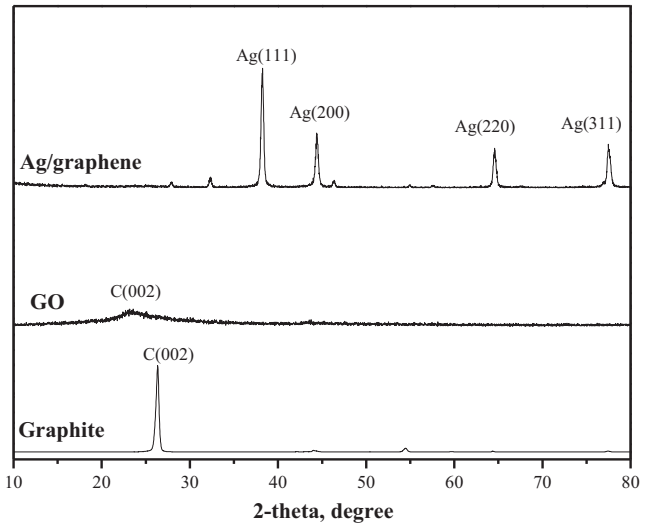

Fig. 3. XRD patterns of graphite, GO and Ag/graphene.

2.3. Batch adsorption experiments

The adsorption of Hg^{2+} on Ag/graphene was studied by batch technique. All batch adsorption experiments were performed by mixing a certain amount of Ag/graphene sorbent into a predeterminated concentration of $HgCl_2$ solution (100 mL) with stirring (300 r/min) at room temperature from 0 to 300 min. Then, the supernatants was separated from the mixture solution by filtration with 0.22 μm microfiltration membrane. The concentration of Hg^{2+} ions remaining in solution was measured by mercury analyzer (RA915, St. Petersburg, Russia). The analyzer was designed based on zeeman effect which has high sensitivity for mercury detection. The effect of several parameters, such as pH, concentrations, contact time and adsorbent dose on the adsorption was also studied. The pH of the adsorptive solutions was adjusted by using sulfuric acid and sodium hydroxide when required. The Hg^{2+} removal efficiency and adsorbing capacities were calculated using the equation:

$$\eta = (C_0 - C_e)/C_0 \times 100\% \quad (1)$$

$$Q_e = (C_0 - C_e) \times V/m \quad (2)$$

where η represents the Hg^{2+} removal efficiency (%), C_0 and C_e are the initial and equilibrium concentrations of Hg^{2+} ($mg{\cdot}L^{-1}$), V is the volume of the solution (mL), Q_e is the adsorbing capacities ($mg{\cdot}g^{-1}$) and m is the mass of Ag/graphene (g).

3. Results and discussion

3.1. Characterization of the Ag/grapheme

The infrared spectra were obtained using FT-IR to identify functional groups of the prepared materials. As shown in Fig. 2, there were few peaks detected in the spectrum of raw graphite. After

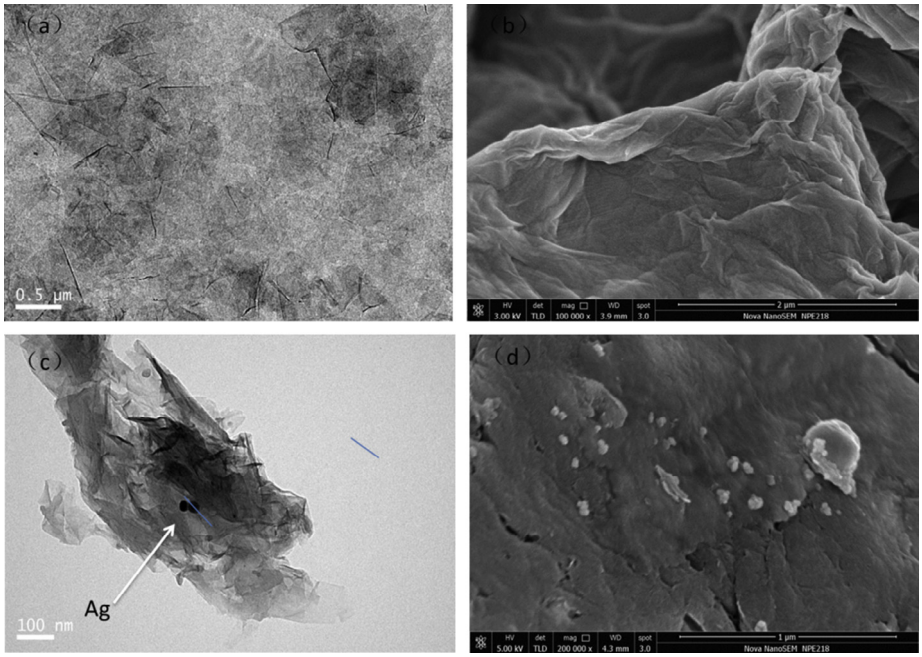

Fig. 4. TEM and SEM micrograph of GO and Ag/graphene.

oxidization, a broad and strong peak around 3216 cm^{-1} corresponds to O–H stretching vibrations of molecular water. The hydroxyl groups was found in the spectrum of GO. Some strong peaks appearing at 1718 and 1624 cm^{-1} were attributed to the C=O stretching vibrations in the carboxyl groups and the C=C vibrations from unoxidized sp^2 C–C bonds, respectively [24]. The peaks at 1158 cm^{-1}, 1038 cm^{-1} and 865 cm^{-1} were attributed to epoxy C–O and alkoxy C–O groups, respectively [25]. While, the peaks of O–H, C=O and C–O almost disappeared in the spectrum of Ag/graphene. Two well-defined peaks at 2850 cm^{-1} and 2919 cm^{-1} were attributed to epoxy CH_2 groups, respectively. These differences indicated that GO was reduced by hydrazine hydrate in the reduction process. In such process, Ag^+ was also reduced to Ag^0 by hydrazine hydrate. However, no Ag–O peak at about 3450 cm^{-1} was detected which meant that Ag atoms may be remained attaching on the surface of graphene sheets [26].

XRD patterns of graphite, GO and Ag/graphene are recorded in Fig. 3. A strong C(002) peak at $2\theta = 26.34°$ was detected in the patterns of raw graphite. It indicated the reflection of a hexagona graphite structure of a carbon material. In the patterns of GO, a broad peak between 21° and 27° was observed which indicated that the formation of oxygen-containing groups and inserted H_2O molecules. Accordingly, part of sp^2 carbons were replaced by these oxygen-containing groups. Meanwhile, the long-range order structure of carbon was destroyed. In the diffraction pattern of the Ag/-graphene, the presence of peaks can be indexed to Ag(111), Ag(200), Ag(220) and Ag(311) diffractions, clearly reflected that the Ag particles were formed on the surface of graphene [27]. From Ag/graphene pattern, no peaks for graphene or graphite appeared which proved that Ag particles on the surface of graphene could inhibit the re-assembly of graphene layers. The BET surface areas of graphite, GO, graphene and Ag/graphene were 6.7, 8.9, 432 and 251 m^2/g, respectively. The large surface area was beneficial for adsorption.

The microstructure of the GO and Ag/graphene could be seen in Fig. 4. As shown in Fig. 4(a), the TEM image of GO was given under a low-resolution. It was obvious that the GO exhibited a two-dimensional sheet morphology. From the SEM image of GO (Fig. 4(b)), the graphene nanosheets were clearly visible. A high magnification TEM image of the Ag/graphene is shown in Fig. 4 (c), Ag particles were distributed on the 2D graphene nanosheets. The average particle size of Ag was about 8–10 nm which is consistent with those numbers calculated from the XRD results by the Scherrer Equation. As shown in Fig. 4(d), Ag particles (white) were distributed on the surface of flexible graphene nanosheets. In the process of chemical reduction by hydrazine hydrate, the Ag^+ cations were reduced to Ag and aggregated to Ag particles. Then, Ag particles were engineered on the surface of graphene.

3.2. Effect of the adsorbent dosage on Hg^{2+} removal

The effect of the amount of Ag/graphene on the removal of Hg^{2+} was investigated. As shown in Fig. 5, the removal efficiency of Hg^{2+} increased from 40.6% to 98.8% after 120 min adsorption when the dosage Ag/graphene sorbent increased from 0.025 g to 0.1 g. Based on the equation, the saturated adsorption capacity of Ag/graphene for Hg^{2+} was about 280.8 mg/g when the sorbent dosage was 0.025 g. The mechanism of Ag/graphene might be attributed to the interaction between Ag particles and Hg^{2+} ions [28]. The graphene sheets offered the huge surface areas for the reaction of Ag and Hg. There was also a mechanism that the oxidation of Ag atoms by Hg^{2+} ions to form a shell of mercury with or without amalgamation on the surface of the nanoparticles. The redox reaction can be described as follows [29]:

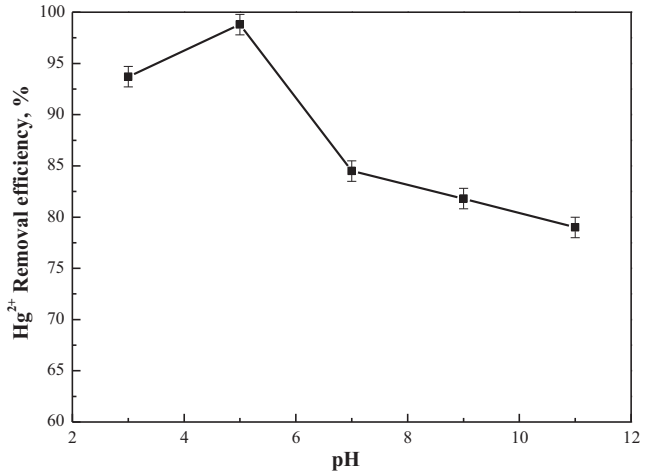

Fig. 6. Effect of initial pH on Hg^{2+} adsorption. Sulfuric acid and sodium hydroxide were used to adjust the pH value a of the solutions. 0.1 g Ag/grapheme sorbent was added into 100 mL of the Hg^{2+} solution (100 mg·L^{-1}) at room temperature with stirring (300r·min^{-1}).

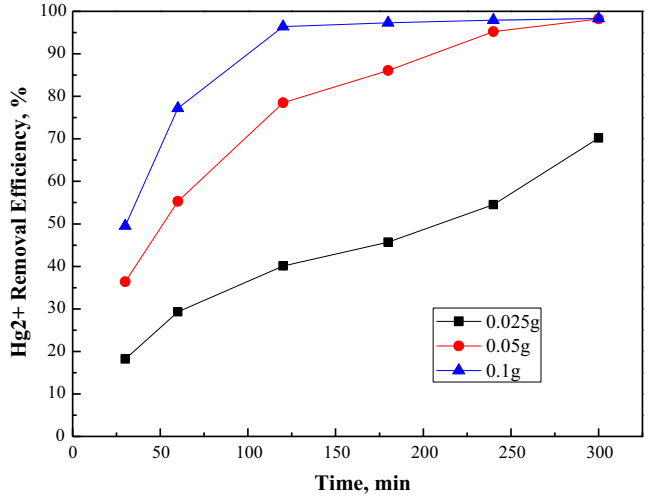

Fig. 5. Effect of the adsorbent dosage on Hg^{2+} removal (pH = 5). Three adsorbent dosages (0.025 g, 0.05 g and 0.1 g) of Ag/graphene were added into 100 mL of the Hg^{2+} solution (100 mg·L^{-1}) at room temperature with stirring (300r·min^{-1}), respectively.

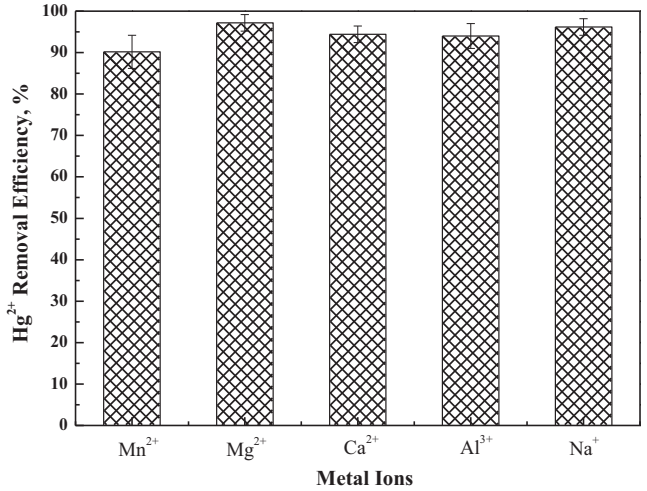

Fig. 7. Effect of co-existed metal ions on Hg^{2+} adsorption (pH = 5). 0.1 g Ag/grapheme sorbent was added into 100 mL of the Hg^{2+} solution (100 mg·L^{-1}) at room temperature with stirring (300r·min^{-1}).

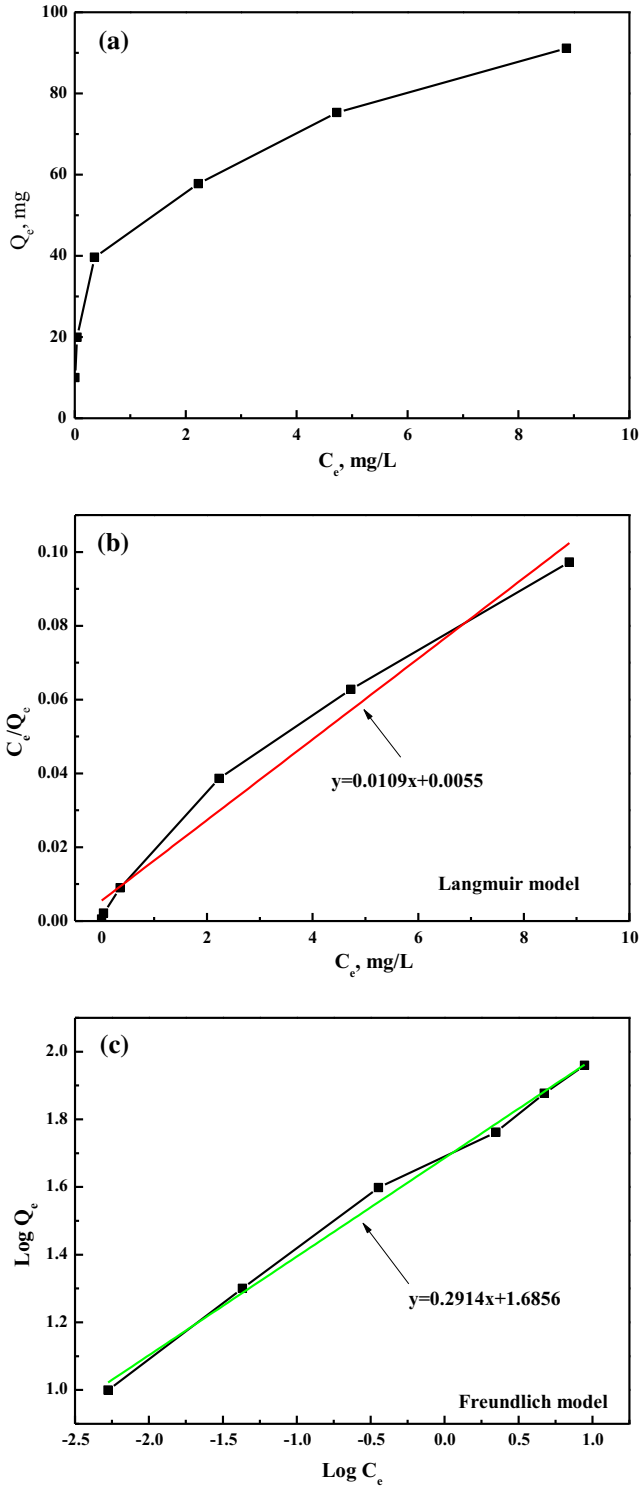

Fig. 8. Adsorption isotherm of Hg^{2+} on Ag/graphene.

Table 1
Values for the Langmuir and Freundlich coefficient for Ag/graphene.

Adsorption isotherm model	Equation parameters	Ag/graphene
Langmuir model	Q_{max} ($mg \cdot g^{-1}$)	91.74
	K_L ($L \cdot mg^{-1}$)	0.5045
	r^2	0.9710
Freundlich model	K_F	5.3957
	1/n	0.2914
	r^2	0.9952

$$Ag(s) + Hg^{2} + (aq) \rightarrow Ag^{+}(aq) + Hg(s) \quad (R1)$$

3.3. Effect of the pH on Hg^{2+} removal

The adsorption performances of Ag/graphene sorbent under different pH value was investigated which were shown in Fig. 6. The Hg^{2+} removal increased from 93.7% to 98.8% when the pH value

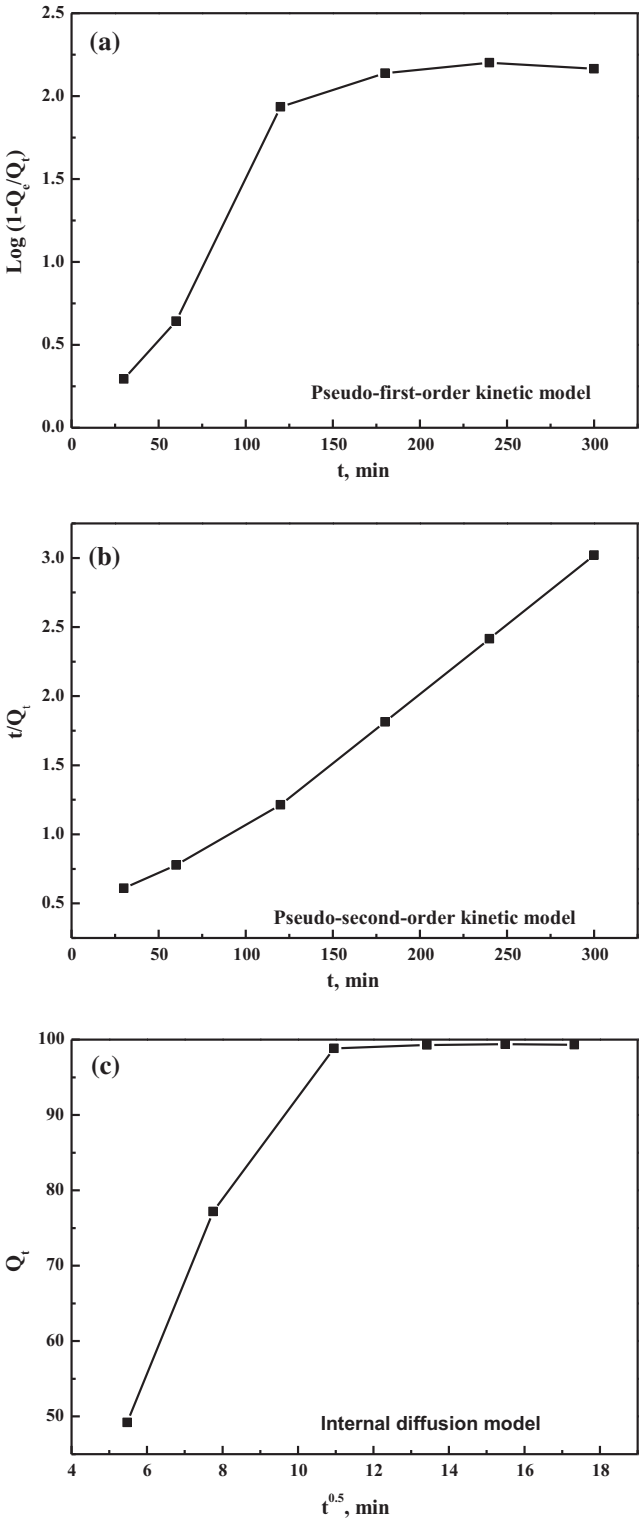

Fig. 9. Adsorption kinetics of Hg^{2+} on Ag/graphene.

increased from 3.0 to 5.0. Then, the Hg^{2+} removal efficiency decreased to 79.0% when the pH value increased to 11.0. The presence of H^+ ions acted as annoying chemicals for the adsorption of Hg^{2+} [30]. It was believed that at high pH, the presence of OH^- greatly increased the possibility of transforming Hg^{2+} to $Hg(OH)^+$, then to $Hg(OH)_2$ [31]. However, $Hg(OH)^+$ and Hg $(OH)_2$ were not benefit for the adsorption. Therefore, the maximum adsorption of mercury within the pH values of 5.0 might be due to partial hydrolysis of Hg^{2+} to $Hg(OH)^+$ and $Hg(OH)_2$ which prevent further hydration process as charge on metal ion decreases.

3.4. Investigation of competitive adsorption by other metal ions

In order to evaluate the adsorption selectivity of Ag/graphene sorbent, it was tested in a mixture solution including some other metal ions (Hg^{2+}, Mn^{2+}, Mg^{2+}, Ca^{2+}, Al^{3+} and Na^+) (Fig. 7). From the Fig. 7, it could be seen that the removal efficiency of Hg^{2+} could get higher than 90% in mixture solution. There is no remarkable influence on the Hg^{2+} removal by Ag/graphene in the present of other metal ions. Thus, Ag/graphene could be a good choice for Hg^{2+} control in many solution conditions.

3.5. Adsorption isotherms

Fig. 8 presents the typical adsorption isotherms of Hg^{2+} on Ag/graphene sorbent at pH of 5.0 in the studied concentration ranges. The obtained isotherm data were fitted using the classical Langmuir model and Freundlich model, respectively. The two typical adsorption isotherms can be expressed as:

$$\text{Langmuir model}: C_e/Q_e = C_e/Q_{max} + 1/(Q_{max} \cdot K_L) \quad (3)$$

Table 2
Values for the kinetic models for Ag/graphene.

Adsorption kinetics model	Equation parameters	Ag/graphene
Pseudo-first-order kinetic model	K_1 (min^{-1})	0.0164
	r_1^2	0.7476
Pseudo-second-order kinetic model	K_2 ($g{\cdot}mg^{-1}{\cdot}min^{-1}$)	0.0003
	r_2^2	0.9935
Internal diffusion model	K_i ($g{\cdot}mg^{-1}{\cdot}min^{-0.5}$)	3.8755
	r_i^2	0.7353

$$\text{Freundlich model}: \text{Log}Q_e = \text{Log}K_F + 1/n \cdot \text{Log}C_e \quad (4)$$

where Q_e is the adsorption capacity (mg/g), C_e is the equilibrated concentration of Hg^{2+} (mg/L), Q_{max} is the saturated adsorption capacity (mg/g), K_L and K_F refer to the affinity parameter of Langmuir sorption constant and Freundlich adsorption capacity, respectively. 1/n is the Freundlich adsorption intensity parameter. The fitting results based on the two isotherm models were shown in Table 1 and Fig. 8. It can be seen that the adsorption of Hg^{2+} on Ag/graphene sorbent was better estimated by the Freundlich model with the correlation coefficient (R^2) in 0.9952 than by the Langmuir model. The fact that the adsorption data of Hg^{2+} were in accordance with the Freundlich model suggests a multilayer adsorption on the heterogenous surface.

3.6. Adsorption kinetics

The adsorption kinetics parameters are key factor for the designing of adsorption reactors in industrial application. The adsorption kinetics of Ag/graphene sorbent were carried out under room temperature for 120 min with an initial Hg^{2+} concentration of 100 $mg{\cdot}L^{-1}$ at a pH of 5.0. The results are shown in Fig. 9.

Pseudo-first-order, Pseudo-second-order, and internal diffusion kinetic models were applied to interpret the adsorption dynamics in order to investigate the mechanisms and processes of the adsorption. These kinetics models are given as follows:

$$\text{Pseudo-first-order kinetic model}: \text{Log}(Q_e - Q_t) = \text{Log}Q_e - k_1 t/2.303 \quad (5)$$

$$\text{Pseudo-second-order kinetic model}: t/Q_t = 1/(k_2 Q_e) + t/Q_e \quad (6)$$

$$\text{Internal diffusion model}: Q_t = k_i t^{0.5} \quad (7)$$

where Q_e is the amount of metal adsorbed at the equilibrium per unit weight of the adsorbent at equilibrium ($mg{\cdot}g^{-1}$), Q_t is the amount of metal adsorbed at t time ($mg{\cdot}g^{-1}$), k_1 is the Pseudo-first-order adsorption rate constant (min^{-1}), k_2 is the Pseudo-second-order adsorption rate constant (g mg^{-1} min^{-1}), k_i is the internal diffusion rate constant (g mg^{-1} $min^{-0.5}$), and r_1^2, r_2^2 and r_i^2

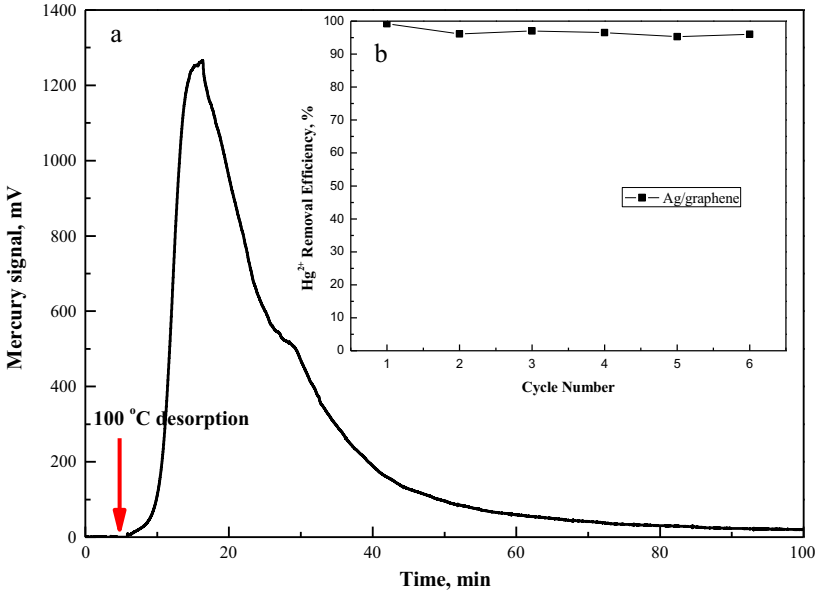

Fig. 10. Regeneration properties of Ag/graphene.

are the corresponding correlation coefficient. The fitting results are shown in Fig. 9 and the values for the kinetic models are shown in Table 2. It was obvious that the Pseudo-second-order kinetic model fitted well with the kinetic data. The r_2^2 was 0.9953, which is better than 0.7476 of r_1^2 and 0.7353 of r_i^2. It is demonstrated that the adsorption mechanism for Hg^{2+} onto Ag/graphene was not the simple physical adsorption.

3.7. Regeneration and reuse

The sorbent regeneration performance of Ag/graphene was evaluated using a thermal decomposition method under 100 °C. The gaseous mercury was detected by CVASS facility. As shown in Fig. 10(a), mercury released quickly from the surface of Ag/graphene. After 100 min thermal desorption, mercury released completely from the sorbent surface. High concentration released mercury could be reclaimed through condensation. Furthermore, to investigate the reusability of the sorbent, 6 cycles of mercury adsorption and desorption tests were performed. The results in Fig. 10(b) showed that the Hg^{2+} removal efficiency would keep higher than 95% even after 6 cycles. Therefore, it was economic to use Ag/graphene as a high efficient sorbent for Hg^{2+} in contaminated water.

4. Conclusions

The Ag/graphene adsorbent was prepared successfully in the proposed method. The analysis by XRD, TEM and SEM showed that Ag particles were engineered on the surface of graphene sheets. According to the adsorption experiments, over 98% Hg^{2+} was removed by 0.1 g Ag/graphene sorbent in 120 min. Large numbers of Ag active sites for Hg^{2+} adsorption were introduced on the graphene sheets. The Hg^{2+} removal efficiency reached a maximum at a pH of 5.0. The co-existed metal ions have no remarkable influence on the adsorption. The best-fit experimental equilibrium data derived from the Freundlich model suggested multilayer coverage and chemisorption of Hg^{2+} onto Ag/graphene. The pseudo-second-order model was the suitable for the adsorption kinetic analysis. Ag/graphene exhibited excellent regeneration performance, mercury could completely released from its surface after thermo-desorption at 100 °C. And the Hg^{2+} removal efficiency remained unchanged after six reuse cycles. Future research on mercury removal can include the investigation of other noble metals, as well as different supports. The capacities for mercury capture by the graphene support and the unsupported silver particles can also be determined in future work. The optimum loading of silver on the support will be determined in future work.

Acknowledgements

This study was supported by the Major State Basic Research Development Program of China (973 Program, No. 2013CB430005) and the National Natural Science Foundation of China (No. 21677096).

References

[1] Tchounwou PB, Ayensu WK, Nisashivili N, Sutton D. Review: environmental exposure to mercury and its toxicopathologic implications for public health. Environ Toxicol 2003;18:149–75.
[2] Mackey TK, Contreras JT, Liang BA. The Minamata convention on mercury: attempting to address the global controversy of dental amalgam use and mercury waste disposal. Sci Total Environ 2014;472:125–9.
[3] Liu MD, Zhang W, Wang XJ, Chen L, Wang HH, Luo Y, et al. Mercury release to aquatic environments from anthropogenic sources in China from 2001 to 2012. Environ Sci Technol 2016;50:8169–77.
[4] Naushad M, Ahamad T, Sharma G, Al-Muhtaseb AH, Albadarin AB, Alam MM, et al. Synthesis and characterization of a new starch/SnO_2 nanocomposite for efficient adsorption of toxic Hg^{2+} metal ion. Chem Eng J 2016;300:306–16.
[5] Qu Z, Yan LL, Li L, Xu JF, Liu MM, Li ZC, et al. Ultraeffective ZnS nanocrystals sorbent for mercury (II) removal based on size-dependent cation exchange. ACS Appl Mater Interfaces 2014;6:18026–32.
[6] Ojea-Jimenez I, Lopez X, Arbiol J, Puntes V. Citrate-coated gold nanoparticles as smart scavengers for mercury(II) removal from polluted waters. ACS Nano 2012;6:2253–60.
[7] Chaturabul S, Srirachat W, Wannachod T, Ramakul P, Pancharoen U, Kheawhom S. Separation of mercury (II) from petroleum produced water via hollow fiber supported liquid membrane and mass transfer modeling. Chem Eng J 2015;265:34–46.
[8] Arshadi M. Manganese chloride nanoparticles: a practical adsorbent for the sequestration of Hg(II) ions from aqueous solution. Chem Eng J 2015;259:170–82.
[9] Patra AK, Kim D. Smart design of self-assembled mesoporous α-FeOOH nanoparticle: high-surface-area sorbent for Hg^{2+} from waste water. ACS Sustain Chem Eng 2017;5:1272–9.
[10] Gong R, Cai W, Li N, Chen J, Liang J, Cao J. Preparation and application of thiol wheat straw as sorbent for removing mercury ion from aqueous solution. Desalin Water Treat 2012;21:274–9.
[11] Taurozzi JS, Redko MY, Manes KM, Jackson JE, Tarabara VV. Microsized particles of Aza222 polymer as a regenerable ultrahigh affinity sorbent for the removal of mercury from aqueous solutions. Sep Purif Technol 2013;116:415–25.
[12] Morris T, Copeland H, McLinden E, Wilson S, Szulczewski G. The effects of mercury adsorption on the optical response of size-selected gold and silver nanoparticles. Langmuir 2002;18:7261–4.
[13] Granite EJ, Pennline HW, Hargis RA. Novel sorbents for mercury removal from flue gas. Ind Eng Chem Res 2000;39:1020–9.
[14] Granite EJ, Myer CR, King WP, Stanko DC, Pennline HW. Sorbents for mercury capture from fuel gas with application to gasification systems. Ind Eng Chem Res 2006;45:4844–8.
[15] Poulston S, Granite EJ, Pennline HW, Myer CR, Stanko DP, Hamilton H, et al. Metal sorbents for high temperature mercury capture from fuel gas. Fuel 2007;86:2201–3.
[16] Baltrus JP, Granite EJ, Stanko DC, Pennline HW. Surface characterization of Pd/Al_2O_3 sorbents for mercury capture from fuel gas. Main Group Chemistry 2008;7:217–225.
[17] Baltrus JP, Granite EJ, Pennline HW, Stanko DC, Hamilton H, Roswell L, et al. Surface characterization of palladium-alumina sorbents for high temperature capture of mercury and arsenic from fuel gas. Fuel 2010;89:1323–5.
[18] Baltrus JP, Granite EJ, Rupp EC, Stanko DC, Howard B, Pennline HW. Effect of palladium dispersion on the capture of toxic components from fuel gas by palladium-alumina sorbents. Fuel 2011;90:1992–8.
[19] Rupp EC, Granite EJ, Stanko DC. Laboratory scale studies of Pd/γ-Al_2O_3 sorbents for the removal of trace contaminants from coal-derived fuel gas at elevated temperatures. Fuel 2010;108:131–6.
[20] Novoselov KS, Geim AK, Morozov SV, Jiang D, Zhang Y, Dubonos SV, et al. Electric field effect in atomically thin carbon films. Science 2004;306:666–9.
[21] Georgakilas V, Otyepka M, Bourlinos AB, Chandra V, Kim VN, Kemp KC, et al. Functionalization of graphene: covalent and non-covalent approaches. Derivatives and applications. Chem Rev 2012;112:6156–214.
[22] Dutta D, Thiyagarajan S, Bahadur D. SnO_2 quantum dots decorated reduced graphene oxide nanocomposites for efficient water remediation. Chem Eng J 2016;297:55–65.
[23] Hummers WS, Offeman RE. Preparation of graphitic oxide. J Am Chem Soc 1958;80. 1339.
[24] Si Y, Samulski ET. Synthesis of water soluble graphene. Nano Lett 2008;8:1679–82.
[25] Murugan AV, Muraliganth T, Manthiram A. Rapid, facile microwave-solvothermal synthesis of graphene nanosheets and their polyaniline nanocomposites for energy storage. Chem Mater 2010;22. 2692-2692.
[26] Hull RV, Li L, Xing YC, Chusuei CC. Pt nanoparticle binding on functionalized multiwalled carbon nanotubes. Chem Mater 2016;18:1780–8.
[27] Shen JF, Shi M, Li N, Yan B, Ma HW, Hu YZ, et al. Facile synthesis and application of Ag-chemically converted graphene nanocomposite. Nano Res 2010;3:339–49.
[28] Yuan CG, Wang JC, Zhai WH, Zhang Y, Zhang YY, Li J, et al. Silver modified magnetic carbon nanotubes composite as a selective solid phase extractor for preconcentration and determination of trace mercury ions in water solution. Int J Environ Anal Chem 2013;93:1513–24.
[29] Yang N, Gao Y, Zhang Y, Shen Z, Wu A. A new rapid colorimetric detection method of Al^{3+} with high sensitivity and excellent selectivity based on a new mechanism of aggregation of smaller etched silver nanoparticles. Talanta 2014;122:272–7.
[30] Kadirvelu K, Kavipriva M, Karthika C, Vennilamani N, Pattabhi S. Mercury (II) adsorption by activated carbon made from sago waste. Carbon 2004;42:745–52.
[31] Asasian N, Kaghazchi T. Optimization of activated carbon sulfurization to reach adsorbent with the highest capacity for mercury adsorption. Sep Sci Technol 2013;48:2059–72.